Zuerst ersch. in : Organometallics ; 28 (2009), 14. - S. 4048 - 4055
DOI : 10.1021/om900198c

Unusual Reactivity of *N*,*N*,*N*′,*N*′-Tetramethylethylenediamine-Coordinated Neutral Nickel(II) Polymerization Catalysts

Andreas Berkefeld, Heiko M. Möller, and Stefan Mecking*

Chair of Chemical Materials Science, Department of Chemistry, University of Konstanz, Universitätsstrasse 10, D-78457 Konstanz, Germany

Tmeda-coordinated species [(N,O)NiCH$_3$(tmeda)] (tmeda = *N*,*N*,*N*′,*N*′-tetramethylethylenediamine), obtained by reaction of [(tmeda)NiMe$_2$] with salicylaldimines, (N^O)H, are reactive and versatile intermediates for olefin polymerization catalysis. Solution NMR spectroscopic studies of **1**-tmeda (N,O = 2,6-(3,5-(F$_3$C)$_2$C$_6$H$_3$)$_2$C$_6$H$_3$-N=CH-(3,5-I$_2$-2-OC$_6$H$_2$)) revealed two major binding modes of the tmeda ligand, open κ^1- and, unexpectedly, chelating κ^2-fashion, which interconvert slowly on the NMR chemical shift time scale, and form equilibria with solvent complexes **1**-L (L = dmso, methanol). Binding of tmeda is favored by 2−3 orders of magnitude at the temperatures studied (25 to 80 °C) over binding of solvent. Chelating κ^2-coordination of tmeda renders the monoanionic bidentate salicylaldiminato ligand κ^1-coordinate. Exposure of dmso solutions of **1**-tmeda to excess ethylene in an NMR tube at 55 °C resulted in the very minor formation of propylene and an equilibrium mixture of Ni(II)-ethyl complexes **2**-dmso and [(κ^1-N,*O*)Ni($^{\alpha}$CH$_2^{\beta}$CH$_3$)(κ^2-tmeda)] (**2**-κ^2-tmeda). Ethylene is primarily dimerized to butenes, which qualitatively parallels the reactivity observed for tmeda-free solutions of **2**-dmso, but tmeda-coordinated Ni(II)-alkyl complexes appeared unreactive, i.e., dormant, toward ethylene. Carrying out the aforementioned reaction under aqueous conditions revealed that hydrolysis of Ni(II)-Me species to methane is a relevant deactivation pathway of the catalyst precursor, which clearly contrasts the reactivity observed in the absence of tmeda. Observed pseudo-first-order rate constants of overall disappearance of **1**-tmeda split into two independent contributions according to $k_{\mathrm{obs,Me,}\mathbf{1}\text{-tmeda}} = k_{\mathrm{ins,Me,}\mathbf{1}\text{-tmeda}} + k_{\mathrm{hydr,}\mathbf{1}\text{-tmeda}}[\mathrm{water}]$, $k_{\mathrm{hydr,}\mathbf{1}\text{-tmeda}} = 1.9 \times 10^{-4}\ \mathrm{M^{-1}\ s^{-1}}$, and $k_{\mathrm{ins,Me,}\mathbf{1}\text{-tmeda}} \approx 2.4 \times 10^{-4}\ \mathrm{M^{-1}\ s^{-1}}$ (∼0.1 M [C$_2$H$_4$]). Determination of activation parameters of the bimolecular elimination of ethane from **1**-tmeda ($\Delta H^{\ddagger} = 97 \pm 7$ kJ mol^{-1} and $\Delta S^{\ddagger} \approx -5$ J mol^{-1} K^{-1}), a generally relevant deactivation mechanism of Ni(II)-methyl complexes, points out that tmeda-coordinated Ni(II)-methyl complexes, despite being inactive toward activation with ethylene, are actively involved in decomposition reactions.

Introduction

Olefin polymerization by complexes of d^8 metals (late transition metals) has been studied intensely in the past decade.[1] A major motivation is the functional group tolerance of these catalysts, by comparison to their much more oxophilic early transition-metal counterparts. Thus, ethylene and 1-olefins can be copolymerized with electron-deficient polar monomers such as acrylates to higher molecular weight polymers.[2,3] Acrylates can be homooligomerized by an insertion mechanism,[4] and polymerizations can be carried out in aqueous emulsions.[5] These studies prompted renewed interest in neutral nickel(II) ethylene polymerization catalysts.[6−9] The perhaps most prominent class of neutral Ni(II) polymerization catalysts are salicylaldiminato complexes.[7] These are versatile catalysts that afford high molecular

*Corresponding author. E-mail: stefan.mecking@uni-konstanz.de.

(1) (a) Ittel, S. D.; Johnson, L. K.; Brookhart, M. *Chem. Rev.* **2000**, *100*, 1169–1203. (b) Gibson, V. C.; Spitzmesser, S. K. *Chem. Rev.* **2003**, *103*, 283–315. (c) Mecking, S. *Angew. Chem., Int. Ed.* **2001**, *40*, 534–540. (d) Mecking, S. *Coord. Chem. Rev.* **2000**, *203*, 325–351. (e) Guan, Z. *Chem.—Eur. J.* **2002**, *8*, 3086–3092. (f) Domski, G. J.; Rose, J. M.; Coates, G. W.; Bolig, A. D.; Brookhart, M. *Prog. Polym. Sci.* **2007**, *32*, 30–92. (g) Berkefeld, A.; Mecking, S. *Angew. Chem., Int. Ed.* **2008**, *47*, 2538–2542.

(2) (a) Johnson, L. K.; Mecking, S.; Brookhart, M. *J. Am. Chem. Soc.* **1996**, *118*, 267–268. (b) Mecking, S.; Johnson, L. K.; Wang, L.; Brookhart, M. *J. Am. Chem. Soc.* **1998**, *120*, 888–899. (c) Johnson, L.; Wang, L.; McLain, S.; Bennett, A.; Dobbs, K.; Hauptman, E.; Ionkin, A.; Ittel, S.; Kunitsky, K.; Marshall, W.; McCord, E.; Radzewich, C.; Rinehart, A.; Sweetman, K. J.; Wang, Y.; Yin, Z.; Brookhart, M. *ACS Symp. Ser.* **2003**, *857*, 131–142. (d) Li, W.; Zhang, X.; Meetsma, A.; Hessen, B. *J. Am. Chem. Soc.* **2004**, *126*, 12246–12247. (e) Popeney, C. S.; Camacho, D. H.; Guan, Z. *J. Am. Chem. Soc.* **2007**, *129*, 10062–10063.

(3) Drent, E.; van Dijk, R.; van Ginkel, R.; van Oort, B.; Pugh, R. I. *Chem. Commun.* **2002**, 744–745.

(4) (a) Guironnet, D.; Roesle, P.; Rünzi, T.; Göttker-Schnetmann, I.; Mecking, S. *J. Am. Chem. Soc.* **2009**, *131*, 422−423. Also cf. (b) Chen, C; Luo, S.; Jordan, R. F. *J. Am. Chem. Soc.* **2008**, *130*, 12892–12893.

(5) (a) Held, A.; Bauers, F. M.; Mecking, S. *Chem. Commun.* **2000**, 301–302. (b) Tomov, A.; Broyer, J.-P.; Spitz, R. *Macromol. Symp.* **2000**, *150*, 53–58. (c) Bauers, F. M.; Mecking, S. *Angew. Chem., Int. Ed.* **2001**, *40*, 3020–3022. (d) Soula, R.; Novat, C.; Tomov, A.; Spitz, R.; Claverie, J.; Drujon, X.; Malinge, J.; Saudemont, T. *Macromolecules* **2001**, *34*, 2022–2026. (e) Göttker-Schnetmann, I.; Korthals, B.; Mecking, S. *J. Am. Chem. Soc.* **2006**, *128*, 7708–7709. (f) Weber, C. H. M.; Chiche, A.; Krausch, G.; Rosenfeldt, S.; Ballauff, M.; Harnau, L.; Göttker-Schnetmann, I.; Tong, Q.; Mecking, S. *Nano Lett.* **2007**, *7*, 2024−2029. Reviews: (g) Claverie, J. P.; Soula, R. *Prog. Polym. Sci.* **2003**, *28*, 619–662. (h) Mecking, S. *Colloid Polym. Sci.* **2007**, *285*, 605–619.

weight polyethylene, are capable of homooligomerization and copolymerization of 1-olefins (also with polar functional groups providing these are separated from the vinyl group by a spacer), and polymerize in aqueous emulsion to afford unique nanoparticles. The degree of branching of ethylene homopolymers, and thus their crystallinity and thermal properties, can be varied over a wide range by remote substituents.[7]

In studies of catalytic polymerizations, neutral or cationic Ni(II)- and Pd(II)-methyl complexes represent versatile well-defined single-component precursors for catalysis and mechanistic studies. Convenient and increasingly utilized reagents for the preparation of neutral M(II)-Me complexes in general are $[(tmeda)M(CH_3)_2]$[10,11] (M = Ni, Pd; tmeda = *N*,*N*,*N*′,*N*′-tetramethylethylenediamine). Reaction with a stoichiometric amount of a monoanionic bidentate ligand in its protonated form, e.g., of free salicylaldimine, (N,O)H, with $[(tmeda)Ni(CH_3)_2]$, results in protonation of one M(II)-methyl moiety to methane and formation of $[(N,O)NiCH_3(tmeda)]$.[6h,p,q,7c−m,12−14] The tmeda ligand is relatively labile, and in the presence of other coordinating species L, the corresponding complexes $[(N,O)NiCH_3(L)]$ can be formed (e.g., L = pyridine, phosphines, primary amines).[7] Due to their reactivity and lability, the tmeda species are also precursors to highly active catalysts.[7g,14a] However, the nature and properties of the $[(N,O)NiCH_3(tmeda)]$ species are unclear. We now report the results of comprehensive NMR studies of this issue.

Results and Discussion

Reactions of $[(tmeda)Ni(CH_3)_2]$ with salicylaldimines (N,O)H proceed straightforwardly and intrinsically introduce the weakly coordinating bidentate ligand *N*,*N*,*N*′,*N*′-tetramethylethylenediamine, tmeda, to the product complexes $[(N,O)NiCH_3(tmeda)]$ (eq 1). The particular salicylaldimine (N,O)H = 2,6-(3,5-$(F_3C)_2C_6H_3)_2C_6H_3$-N=CH-(3,5-I_2-2-OH-C_6H_2) was chosen for this study, as Ni(II) complexes of this ligand are long-lived, robust, and very active precatalysts for ethylene polymerization.[5e,5f,7h,13]

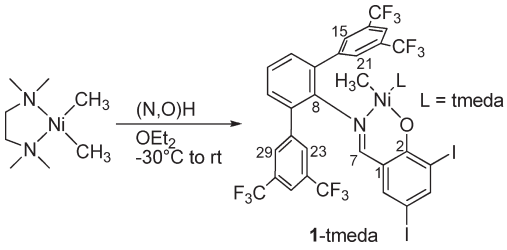

(1)

Polymerization experiments carried out at precatalyst loadings of 1 μmol of **1**-tmeda in toluene solution at 20 °C revealed that overall catalytic activities (measured in units of mol(C_2H_4) mol(**1**-tmeda)$^{-1}$ h^{-1} = TO h^{-1}) are nearly independent of the ethylene concentration in the pressure range from 10 bar (3.0×10^4 TO h^{-1}) to 30 bar (3.4×10^4 TO h^{-1}). This indicates that under these conditions tmeda does not compete with monomer binding to the metal center. A highly linear semicrystalline polyethylene is obtained, with, for example, a molecular weight of $M_n = 1.5 \times 10^5$ g mol^{-1} ($M_w/M_n = 2.5$, ca. 50% crystallinity; prepared at 30 bar).

^{1}H NMR Spectroscopic Studies of 1-tmeda. Two Ni(II)-methyl species coexist in a close to 1:1 ratio in dmso-d_6 solutions of **1**-tmeda at ambient temperatures. Characteristic

(6) (a) Braunstein, P.; Pietsch, J.; Chauvin, Y.; Mercier, S.; Saussine, L.; DeCian, A.; Fischer, J. *J. Chem. Soc., Dalton Trans.* **1996**, 3571–3574. (b) Braunstein, P.; Pietsch, J.; Chauvin, Y.; DeCian, A.; Fischer, J. *J. Organomet. Chem.* **1997**, *529*, 387–393. (c) Pietsch, J.; Braunstein, P.; Chauvin, Y. *New J. Chem.* **1998**, *22*, 467–472. (d) Rachita, M. J.; Huff, R. L.; Bennett, J. L.; Brookhart, M. *J. Polym. Sci. Part A* **2000**, *38*, 4627–4640. (e) Hicks, F. A.; Brookhart, M. *Organometallics* **2001**, *20*, 3217–3219. (f) Soula, R.; Broyer, J. P.; Llauro, M. F.; Tomov, A.; Spitz, R.; Claverie, J.; Drujon, X.; Malinge, J.; Saudemont, T. *Macromolecules* **2001**, *34*, 2438–2442. (g) Gibson, V. C.; Tomov, A.; White, A. J. P.; Williams, D. J. *Chem. Commun.* **2001**, 719–720. (h) Schröder, D. L.; Keim, W.; Zuideveld, M. A.; Mecking, S. *Macromolecules* **2002**, *35*, 6071–6073. (i) Hicks, F. A.; Jenkins, J. C.; Brookhart, M. *Organometallics* **2003**, *22*, 3533–3545. (j) Heinicke, J.; Köhler, M.; Peulecke, N.; He, M.; Kindermann, M. K.; Keim, W.; Fink, G. *Chem.—Eur. J.* **2003**, *9*, 6093–6107. (k) Jenkins, J. C.; Brookhart, M. *J. Am. Chem. Soc.* **2004**, *126*, 5827–5842. (l) Speiser, F.; Braunstein, P.; Saussine, L. *Acc. Chem. Res.* **2005**, *38*, 784–793. (m) Zhang, L.; Brookhart, M.; White, P. S. *Organometallics* **2006**, *25*, 1868–1874. (n) Kuhn, P.; Sémeril, D.; Jeunesse, C.; Matt, D.; Neuburger, M.; Mota, A. *Chem.—Eur. J.* **2006**, *12*, 5210–5219. (o) Nowack, R. J.; Hearley, A. K.; Rieger, B. *Z. Anorg. Allg. Chem.* **2005**, *631*, 2775–2781. (p) Yu, S.-M.; Berkefeld, A.; Göttker-Schnetmann, I.; Müller, G.; Mecking, S. *Macromolecules* **2007**, *40*, 421–428. (q) Guironnet, D.; Rünzi, T.; Göttker-Schnetmann, I.; Mecking, S. *Chem. Commun.* **2008**, 4965–4967. (r) Lavanant, L.; Rodriguez, A.-S.; Kirillov, E.; Carpentier, J.-F.; Jordan, R. F. *Organometallics* **2008**, *27*, 2107–2117. (s) Rodriguez, B. A.; Delferro, M.; Marks, T. J. *Organometallics* **2008**, *27*, 2166–2168. (t) Azoulay, J. D.; Itigaki, K.; Wu, G.; Bazan, G. C. *Organometallics* **2008**, *27*, 2273–2280. (u) Zhou, X.; Bontemps, S.; Jordan, R. F. *Organometallics* **2008**, *27*, 4821–4824.

(7) (a) Johnson, L. K.; Bennett, A. M. A.; Ittel, S. D.; Wang, L.; Parthasarathy, A.; Hauptman, E.; Simpson, R. D.; Feldman, J.; Coughlin, E. B. (DuPont) WO98/30609, **1998**. (b) Wang, C.; Friedrich, S.; Younkin, T. R.; Li, R. T.; Grubbs, R. H.; Bansleben, D. A.; Day, M. W. *Organometallics* **1998**, *17*, 3149–3151. (c) Younkin, T. R.; Connor, E. F.; Henderson, J. I.; Friedrich, S. K.; Grubbs, R. H.; Bansleben, D. A. *Science* **2000**, *287*, 460–462. (d) Connor, E. F.; Younkin, T. R.; Henderson, J. I.; Hwang, S.; Grubbs, R. H.; Roberts, W. P.; Litzau, J. J. *J. Polym. Sci. Part A* **2002**, *40*, 2842–2854. (e) Connor, E. F.; Younkin, T. R.; Henderson, J. I.; Waltman, A. W.; Grubbs, R. H. *Chem. Commun.* **2003**, 2272–2273. (f) Darensbourg, D. J.; Ortiz, C. G.; Yarbrough, J. C. *Inorg. Chem.* **2003**, *42*, 6915–6922. (g) Bastero, A.; Kolb, L.; Wehrmann, P.; Bauers, F. M.; Göttker gen. Schnetmann, I.; Monteil, V.; Thomann, R.; Chowdhry, M. M.; Mecking, S. *Polym. Mat. Sci. Eng.* **2004**, *90*, 740–741. (h) Zuideveld, M. A.; Wehrmann, P.; Röhr, C.; Mecking, S. *Angew. Chem., Int. Ed.* **2004**, *43*, 869–873. (i) Wehrmann, P.; Mecking, S. *Macromolecules* **2006**, *39*, 5963–5964. (j) Wehrmann, P.; Zuideveld, M. A.; Thomann, R.; Mecking, S. *Macromolecules* **2006**, *39*, 5995–6002. (k) Göttker Schnetmann, I.; Wehrmann, P.; Röhr, C.; Mecking, S. *Organometallics* **2007**, *26*, 2348–2362. (l) Bastero, A.; Göttker-Schnetmann, I.; Röhr, C.; Mecking, S. *Adv. Synth. Catal.* **2007**, *349*, 2307–2316. (m) Wehrmann, P.; Mecking, S. *Organometallics* **2008**, *27*, 1399−1408. Also see: (n) Brasse, M.; Campora, J.; Palma, P.; Alvarez, E.; Cruz, V.; Ramos, J.; Reyes, M. L. *Organometallics* **2008**, *27*, 4711–4723.

(8) For early related work on phosphino enolate catalyst systems see: (a) Keim, W.; Kowaldt, F. H.; Goddard, R.; Krüger, C. *Angew. Chem., Int. Ed. Engl.* **1978**, *17*, 466–467. (b) Ostoja Starzewski, K. A.; Witte, J. *Angew. Chem., Int. Ed. Engl.* **1985**, *24*, 599–601. (c) Klabunde, U.; Ittel, S. D. *J. Mol. Catal.* **1987**, *41*, 123–134.

(9) For computational studies see: (a) Chan, M. S. W.; Deng, L.; Ziegler, T. *Organometallics* **2000**, *19*, 2741–2750. (b) Zeller, A.; Strassner, T. *J. Organomet. Chem.* **2006**, *691*, 4379–4385.

(10) Kaschube, W.; Pörschke, K. R.; Wilke, G. *J. Organomet. Chem.* **1988**, *355*, 525–532.

(11) de Graaf, W.; Boersma, J.; Smeets, W. J. J.; Spek, A. L.; van Koten, G. *Organometallics* **1989**, *8*, 2907–2917.

(12) For $[(Me_3P)_2NiMe(OMe)]$ as a precursor see: Klein, H.-F. *Inorg. Chim. Acta* **1996**, *248*, 111–114.

(13) Berkefeld, A.; Mecking, S. *J. Am. Chem. Soc.* **2009**, *131*, 1565–1574.

(14) For a corresponding reaction of $[(tmeda)PdMe_2]$ with salicylaldimine: ref 7f. With (zwitterionic) phosphinosulfonic acids, (P,O)H: (a) Skupov, K. M.; Marella, P. R.; Simard, M.; Yap, G. P. A.; Allen, N; Conner, D.; Goodall, B. L.; Claverie, J. P. *Macromol. Rapid Commun.* **2007**, *28*, 2033–2038. (b) Vela, J.; Lief, G. R.; Shen, Z.; Jordan, R. F. *Organometallics* **2007**, *26*, 6624–6635 and ref 4a.

Scheme 1. Equilibrium between 1-κ^2-tmeda and 1-dmso As Observed by NMR Spectroscopy

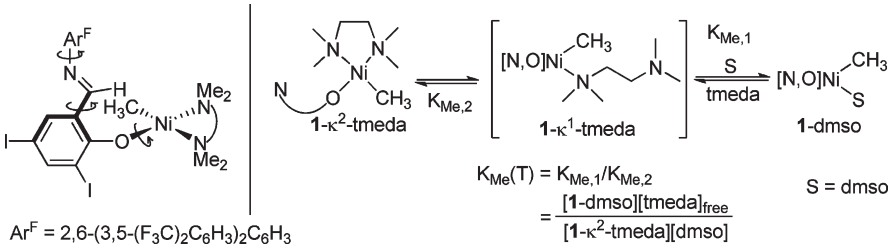

low- and high-field ^{1}H NMR resonances of the imine (−*H*C=N−, H_7, see eq 1) and Ni(II)-CH_3 protons, respectively, were observed at 11.08 and −1.79 ppm for the first and at 8.11 and −1.19 ppm for the second Ni(II)-methyl species (Figure S1, Supporting Information (SI)). Two-dimensional rotating-frame nuclear Overhauser effect spectroscopy (2D ROESY) indicates the chemical exchange of both the imine and the Ni(II)-methyl protons, respectively, between the two species (Figure S2, SI). The exchange occurs slowly on the NMR chemical shift time scale. By contrast to NMR spectra of **1**-tmeda, a single defined Ni(II)-methyl species is observed for the separately prepared[13] dmso-coordinated complex [(N,O)NiCH$_3$(dmso)] (**1**-dmso), and characteristic ^{1}H NMR resonances of the imine and Ni(II)-CH_3 protons were observed at 8.13 and −1.19 ppm, respectively. Notably, the addition of 1 equiv of tmeda to a dmso-d_6 solution of neat **1**-dmso resulted in a ^{1}H NMR spectrum entirely identical to that observed for **1**-tmeda in dmso-d_6, consistent with the partial ligand exchange of (deuterated) dmso by tmeda and the formation of a tmeda-coordinated Ni(II)-methyl complex. Further, the Ni(II)-methyl species observed at −1.79 ppm became the dominant species (with a molar fraction $x > 0.9$) after the addition of 3 equiv of tmeda to either sample (Figure S3, SI), which shifts the equilibrium concentrations between dmso- and tmeda-coordinated Ni(II)-methyl complexes in favor of the latter.

^{1}H NMR, and 2D ROESY data in particular, reveal the coordination of tmeda to the Ni(II)-alkyl moiety to occur preferentially in a κ^2-fashion with the salicylaldiminato ligand κ^1-coordinated (**1**-κ^2-tmeda, Scheme 1) in dmso-d_6 solution, surprisingly. This coordination mode contrasts with the known observation that tmeda can be facily replaced from [(N,O)NiMe(tmeda)] species by ligands such as L= pyridine or phosphine to afford the κ^2-salicylaldiminato complexes [(N,O)NiMe(L)].[7c,e,f,h,k−m] This unexpected structure is clearly evident from, first, the κ^2-coordination of tmeda in **1**-κ^2-tmeda rendering the N-CH_3 groups inequivalent, and distinct ^{1}H NMR resonances were observed at 2.36, 2.01, 1.82, and 1.64 ppm (Figure S1, SI). 2D ROESY data indicate that the N-methyl groups of the κ^2-tmeda ligand are subject to (i) self-exchange and (ii) exchange with free tmeda from solution. Both processes proceed slowly on the NMR chemical shift time scale. Distinct dipolar proton−proton couplings of all four N-methyl to the imine and Ni(II)-methyl protons as well as to the four ortho protons of the trifluoromethyl-substituted phenyl rings of the terphenylaniline unit 2,6-(3,5-(F$_3$C)$_2$C$_6H_3$)$_2$C$_6$H$_3$ (Figure S2, SI) are in agreement with unhindered rotation around the C_1-C_7 and $N-C_8$ bond (C_1−HC_7=N−C_8, see Scheme 1). Second, particular cross-peaks were observed by 2D ROESY consistent with dipolar coupling of Ni(II)-methyl and imine protons for **1**-κ^2-tmeda (Figure S2, SI). Notably, κ^2-coordination of the (N,O)-ligand in complexes [(N,O)NiCH$_3$(L)] (with, e. g., L = dmso) enforces the opposite spatial orientation of the Ni(II)-methyl and imine moieties and, as a consequence, no NOEs between these protons have been observed for these complexes. The relative orientation of the Ni(II)-methyl and imine moiety toward each other reveals further evidence of an unhindered rotation around the $N-C_8$ and C_1-C_7 bonds in **1**-κ^2-tmeda. In particular, rotation around the C_1-C_7 bond is indicative of a κ^1-O-coordination of the (N,O)-ligand and, third, is assumed to cause the significant low-field shift of the imine ^{1}H NMR resonance detected at 11.08 ppm as opposed to 8.13 ppm observed for **1**-dmso and 8.08 ppm in the case of the free salicylaldimine (N,O)H. The complete ^{1}H and ^{13}C NMR spectroscopic assignment of **1**-κ^2-tmeda is provided in the Experimental Section.

The equilibrium constant $K_{Me}(T) = [\mathbf{1}\text{-dmso}][\text{tmeda}]_{free}/([\mathbf{1}\text{-}\kappa^2\text{-tmeda}][\text{dmso}])$ was determined in the temperature range from 27 to 80 °C by ^{1}H NMR spectroscopy. The formation of **1**-κ^2-tmeda is thermodynamically favored over the solvent species **1**-dmso; values of $K_{Me}(T)$ increased from 2.9×10^{-3} to 4.0×10^{-2} over the temperature range studied (27 to 80 °C). Linear regression of a plot of $\ln(K_{Me}(T))$ vs reciprocal temperatures provided a reaction enthalpy $\Delta H°$ of 44 ± 1 kJ mol^{-1}, and a difference of the free enthalpies of **1**-κ^2-tmeda and **1**-dmso, $\Delta G° = 15$ kJ mol^{-1}, was calculated from $K_{Me}(T)$ at room temperature (Figure S4, SI).

Presumably, **1**-κ^2-tmeda and **1**-dmso equilibrate via the Ni(II)-methyl species **1**-κ^1-tmeda (Scheme 1). The latter was not observed in dmso-d_6 solution, but studies of **1**-tmeda in methanol-d_4 and toluene-d_8 solution revealed that complex **1**-κ^1-tmeda is a relevant species. Values for the equilibrium constant $K_{Me,2} = [\mathbf{1}\text{-}\kappa^2\text{-tmeda}]/[\mathbf{1}\text{-}\kappa^1\text{-tmeda}]$ were found to range from 0.66 ($\Delta G° = 1.0$ kJ mol^{-1}) in methanol-d_4 to 0.88 ($\Delta G° = 0.3$ kJ mol^{-1}) in toluene-d_8 solution at 25 °C, providing a measure for the competition of the formation of the (five-membered) κ^2-tmeda chelate vs the (six-membered) κ^2-salicylaldiminato chelate.[15,16]

(15) Key ^{1}H NMR resonances observed in methanol-d_4 at 25 °C: 10.19 and −1.64 (−*H*C=N− and Ni(II)-CH_3, **1**-κ^2-tmeda); 7.69, 2.40, 2.32, and −0.72 (−*H*C=N−, {(*H*$_3$C)$_2$NCH$_2$}$_{1/2}$, {(H$_3$C)$_2$NC*H*$_2$}$_{1/2}$, and Ni(II)-CH_3, **1**-κ^1-tmeda); 7.62 and −1.28 (−*H*C=N− and Ni(II)-CH_3, **1**-O(D)CD$_3$) ppm. Resonances of free tmeda were observed at 2.01 ({(*H*$_3$C)$_2$NCH$_2$}$_{1/2}$) and 2.26 ({(H$_3$C)$_2$NC*H*$_2$}$_{1/2}$) ppm. Equilibrium constants according to ^{1}H NMR spectra (see Scheme 1): $K_{Me,1} = 5.3 \times 10^{-3}$ ($\Delta G° = 13$ kJ mol^{-1}), $K_{Me} = K_{Me,1}/K_{Me,2} = 8 \times 10^{-3}$ ($\Delta G° = 14$ kJ mol^{-1}). Key ^{1}H NMR resonances (imine/Ni(II)-C*H*$_3$) of **1**-κ^2-tmeda and **1**-κ^1-tmeda observed in toluene-d_8 at 25 °C: 11.80/−1.45 and 8.88/−1.39 ppm, respectively. A third Ni(II)-methyl species detected at −1.29 ppm (Ni(II)-CH_3, $x = 0.21$) was tentatively assigned to the tmeda-bridged bimolecular complex [{(N,O)NiCH$_3$}$_2$(μ^2-tmeda)] (**1**-μ^2-tmeda), consistent with the resonances of half an equivalent of free tmeda being observed in the toluene-d_8 solution.

(16) The stepwise addition of *N,N*-dimethylbutylamine to solutions of **1**-tmeda in dmso-d_6 (15 mM; 1.2 equiv amine) or methanol-d_4 (6 mM; 19 equiv amine) did not yield observable quantities of the corresponding κ^1-amine complex [(N,O)NiCH$_3$(N(Me)$_2$C$_4$H$_9$)], an observation that underlines the particular binding properties of the bidentate tmeda ligand.

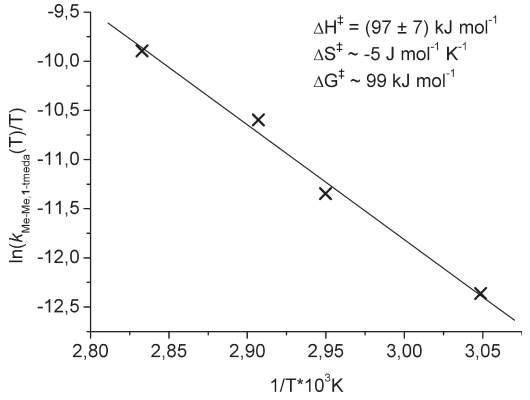

Figure 1. Eyring plot of second-order rate constants $k_{\text{Me-Me, 1-tmeda}}(T)$ for the decomposition of **1**-tmeda to C_2H_6 in dmso-d_6 solution (as determined from the decrease of the total Ni(II)-CH_3 integral in the temperature range from T = 55 to 80 °C).

Scheme 2. Proposed Mechanism of Ethane Formation via the Bimolecular Coupling of Ni(II)-Methyl Moieties[a]

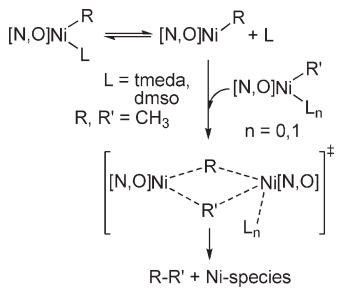

[a] L = tmeda may represent both κ^1- and κ^2-tmeda Ni(II)-methyl species.

Decomposition of Ni(II)-Methyl Species. A relevant decomposition pathway specific to Ni(II)-methyl complexes is the bimolecular homocoupling of Ni(II)-methyl moieties to ethane. The temperature dependence of second-order rate constants $k_{\text{Me-Me}}(T)$ of ethane formation from neat **1**-dmso determined by variable-temperature ^{1}H NMR spectroscopic monitoring yielded the activation parameters $\Delta H^{\ddagger} = 57 \pm 1$ kJ mol^{-1} and $\Delta S^{\ddagger} = -(129 \pm 2)$ J mol^{-1} K^{-1}, corresponding to $\Delta G^{\ddagger}(298\text{ K}) = 95 \pm 1$ kJ mol^{-1}.[13] In agreement with the assumed formation of a dinuclear nickel species in the rate-determining step of ethane formation, the activation entropy was found to particularly contribute to the free activation enthalpy. Analogous kinetic studies of the decomposition of **1**-tmeda to ethane[17] (Figure S5, SI) revealed a similar free activation enthalpy $\Delta G^{\ddagger}(298\text{ K}) \approx 99$ kJ mol^{-1} but considerably different activation parameters $\Delta H^{\ddagger} = 97 \pm 7$ kJ mol^{-1} and $\Delta S^{\ddagger} \approx -5$ J mol^{-1} K^{-1} (Figure 1).

A tentative explanation for this observation is that the required breaking of the Ni(II)−N bond(s) to tmeda accounts for the relatively higher activation enthalpy. This is, however, partially compensated by an overall activation entropy, which is quite high (low negative value) given the bimolecular nature of the overall reaction (Scheme 2). The specific bidentate property of tmeda by comparison to dmso apparently affects the rate-determining step. Possibly, dissociation of the five-ring κ^2-tmeda chelate (the rigidity of which is also evidenced by its NMR spectroscopic properties, see above), which results in a gain of conformational degrees of freedom, occurs in a concerted fashion with the rate-determining step of the deactivation reaction. The potential bridging coordination of tmeda may also affect the bimolecular reaction.

Reactivity of 1-tmeda toward Ethylene and Water in dmso Solution. Chain growth by ethylene insertion is a key step in the utilization of salicylaldiminato complexes as polymerization catalysts. Exposure of dmso-d_6 solutions of **1**-tmeda (15−30 mM) to ethylene (~0.1−0.2 M) in an NMR tube at T = 55 °C resulted in the partial reaction of **1**-dmso and **1**-κ^2-tmeda to form propylene and Ni(II)-ethyl species (at an overall conversion of Ni(II)-Me ≤ 10%). The latter are the resting state of catalytic ethylene dimerization to butenes, which results in gradual consumption of ethylene. This qualitatively parallels the behavior reported previously[13] for tmeda-free solutions of **1**-dmso toward ethylene in dmso. In the latter case, propylene was formed with a pseudo-first-order rate $k_{\text{ins,Me}} = (6.8 \pm 0.3) \times 10^{-4}$ s^{-1} (at 0.15 M ethylene), and the Ni(II)-ethyl complex [(N,O)Ni-($^{\alpha}CH_2^{\beta}CH_3$)(dmso)] (**2**-dmso) catalyzed the conversion of ethylene to butenes. **2**-dmso is subject to interconversion of the $^{\alpha}$C and $^{\beta}$C moieties via an intermediate [(N,O)NiH-(ethylene)] complex, which occurs slowly on the NMR chemical shift time scale.[13]

^{1}H NMR resonances of the Ni(II)-alkyl species considerably sharpened upon cooling of the sample to room temperature and revealed the presence of a second Ni(II)-ethyl species in a close to 1:1 equilibrium mixture with **2**-dmso (Figure 2). Characteristic ^{1}H and ^{13}C NMR resonances (^{13}C chemical shifts were detected indirectly by 2D heteronuclear single-quantum correlation (HSQC) spectroscopy) of the new Ni(II)-ethyl species were observed at 11.71 and ~161 (−*HC*=N−), −0.39 (triplet, $^3J_{\text{H-H}} = 7.2$ Hz) and 13.5 (Ni(II)-CHH*CH*$_3$), and −0.89/−1.02 (as broad multiplets each) and −1.5 (Ni(II)-*CHH*CH$_3$) ppm. By comparison to the NMR spectroscopic data obtained for **1**-κ^2-tmeda, the Ni(II)-ethyl species was assigned as the κ^2-tmeda-coordinated complex **2**-κ^2-tmeda on the basis of the significant low-field shift of the imine resonance observed at 11.71 ppm as opposed to 8.21 ppm for **2**-dmso, and the inequivalence of the α-methylene protons [(N,O)Ni(C*H*$^{\alpha}$*H*$^{\alpha'}$CH$_3$)(κ^2-tmeda)] (Figure S6, SI). The very low degree of conversion of **1**-tmeda into **2**-κ^2-tmeda (≤5%) unfortunately precluded detection of the corresponding resonances of the tmeda-ligand in both ^{1}H and 2D NMR spectra.

The α-methylene protons of **2**-κ^2-tmeda are subject to interconversion, as monitored in the temperature regime of slow exchange by 2D ROESY and nuclear Overhauser effect spectroscopy (NOESY) methods. Notably, the interconversion of $^{\alpha}$C and $^{\beta}$C moieties of **2**-κ^2-tmeda appears to proceed very slowly (if at all), and no indicative exchange cross-peaks were observed by 2D NOESY or ROESY as opposed to the dynamics of **2**-dmso. However, positive cross-peaks between the β-methyl proton resonances indicate that a slow ligand exchange occurs between **2**-dmso and **2**-κ^2-tmeda (Scheme 3, Figure S7, SI).[18] As observed for Ni(II)-methyl species

(17) Second-order rate constants $k_{\text{Me-Me,1-tmeda}}(T)$ were determined by ^{1}H NMR spectroscopic monitoring of the time-dependent decrease of the total Ni(II)-CH_3 integral of **1**-tmeda (as the sum of **1**-κ^2-tmeda and **1**-dmso) for temperatures from 55 to 80 °C (Figure S5).

(18) According to the exchange cross-peaks observed, the interconversion of $^{\alpha}$C and $^{\beta}$C moieties of **2**-dmso and the ligand exchange with **2**-κ^2-tmeda apparently occur at similar rates on the time scale of the mixing times τ_{mix} applied in the 2D spectra.

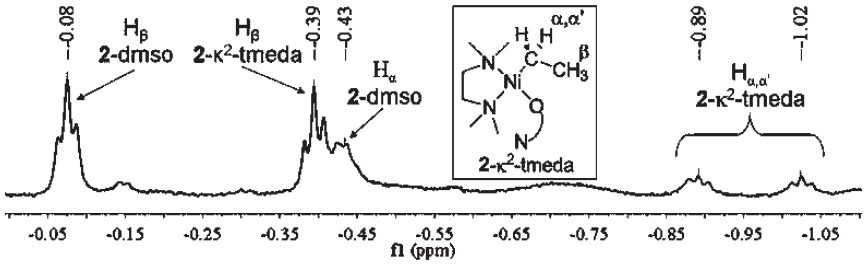

Figure 2. Typical high-field ^{1}H NMR chemical shift region of Ni(II)-alkyls **2**-dmso and **2**-κ^2-tmeda prepared in an NMR tube in dmso-d_6 at T = 55 °C (spectrum shown acquired at 25 °C).

Scheme 3. Dynamic Processes of 2-dmso and 2-κ^2-tmeda Observed by 2D ROESY at T = 25 °C

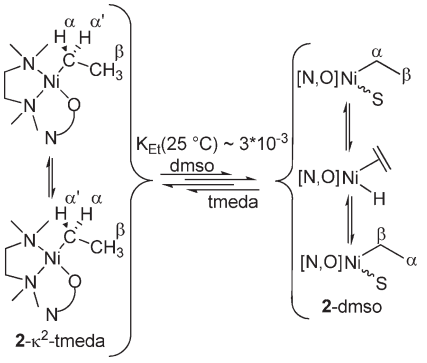

(see above), tmeda has a considerably higher binding affinity toward the Ni(II)-ethyl species than dmso, and a value of $\sim 3 \times 10^{-3}$ was estimated for the equilibrium constant $K_{Et}(T) =$ [**2**-dmso][tmeda]$_{free}$/([**2**-κ^2-tmeda][dmso]) from the ^{1}H NMR spectra at 25 °C.

Kinetic studies of the overall ethylene insertion into the metal−carbon bond of the precursor Ni(II)-methyl species were carried out to survey the reactivity of Ni(II)-alkyls [{κ^1-N,*O*}NiR(κ^2-tmeda)], R ≥ CH_3, in the catalytic C−C linkage of olefins. In this context, the reactivity of **1**-tmeda toward the most ubiquitous polar reagent, water (D_2O), was also addressed. Solutions of **1**-tmeda in dmso-d_6 (34 mM) were exposed to ethylene (~0.1 M) at T=55 °C in the NMR tube, and the time-dependent decrease of the total Ni(II)-methyl integral was monitored by ^{1}H NMR spectroscopy. Apparent pseudo-first-order rate constants $k_{obs,Me,\mathbf{1}\text{-tmeda}}$ were determined by linear regression of plots of ln([**1**-tmeda]$_t$/[**1**-tmeda]$_{t=0}$) vs time (Figure 3).

Unexpectedly, apparent rate constants $k_{obs,Me,\mathbf{1}\text{-tmeda}}$ increased in the presence of increasing amounts of added water (D_2O) in the reaction medium. For example, a value of 6.0×10^{-4} s^{-1} was determined in the presence of 60 equiv of added water (data set (+), Figure 3) as opposed to 2.1×10^{-4} s^{-1} in the absence of water. According to the ^{1}H NMR spectra considerable amounts of CH_3D gradually formed from Ni(II)-methyl bond hydrolysis of **1**-tmeda in the presence of water (D_2O) and ethylene under reaction conditions (catalytic dimerization of ethylene to butenes). Initial rates of methane formation from **1**-tmeda (r_{CH3D}) were determined by ^{1}H NMR spectroscopic monitoring of the gradual growth of the characteristic 1:1:1 triplet resonance of CH_3D (observed at 0.16 ppm) as a function of [D_2O] (for kinetic plots see Figure S8, SI). Linear regression of a plot of $\log_{10}(r_{CH3D})$ vs $\log_{10}([D_2O])$ ([D_2O] = 0.69, 1.38, and 2.12 M) yielded a reaction order with respect to water of 1.2 ± 0.1 (from the slope), consistent with the rate law $r_{CH3D} = k_{hydr,\mathbf{1}\text{-tmeda}}$[**1**-tmeda][$D_2O$]. A pseudo-first-order rate constant of CH_3D formation $k_{CH3D} = 6.3 \times 10^{-6}$ s^{-1} was determined from the y-intercept (Figure 4), corresponding to a second-order rate constant $k_{hydr,\mathbf{1}\text{-tmeda}} = 1.9 \times 10^{-4}$ M^{-1} s^{-1} (for [**1**-tmeda]$_{t=0}$ = 34 mM).[19]

That hydrolysis occurs to a significant extent contrasts the behavior of the analogous tmeda-free system,[13] for which hydrolysis could be detected under appropriate conditions, but only represents a minor reaction pathway (only trace amounts of CH_3D gradually formed under otherwise identical reaction conditions). Apparently, tmeda species are actively involved in hydrolysis reactions. Presumably, the hydrogen-bonding capability of free amines is relevant in this context. For example, hydrogen bonding of water to the noncoordinated amine group in the intermediately occurring **1**-κ^1-tmeda may promote the coordination of water and hydrolysis reactions.

Consideration of $k_{hydr,\mathbf{1}\text{-tmeda}}$ in the calculation of pseudo-first-order insertion rate constants $k_{ins,Me,\mathbf{1}\text{-tmeda}}$ (corrected for hydrolysis) from the kinetic data determined in the presence of water according to $k_{obs,Me,\mathbf{1}\text{-tmeda}} = k_{ins,Me,\mathbf{1}\text{-tmeda}} + k_{hydr,\mathbf{1}\text{-tmeda}}[D_2O]$ yielded $k_{ins,Me,\mathbf{1}\text{-tmeda}} \approx 2.6 \times 10^{-4}$ s^{-1} (as the average calculated for different concentrations of D_2O in the range from 0.69 to 1.38 and 2.12 M), which is equivalent to the value determined in the absence of added water (2.1×10^{-4} s^{-1}) within experimental accuracy.

Concerning the activation of salicylaldiminato Ni(II)-Me species for catalysis, by comparison to a tmeda-free system, the presence of tmeda results in a retardation due to equilibrium formation of **1**-κ^2-tmeda, which itself apparently is dormant for insertion of ethylene.[20] At the same time, however, the κ^2-tmeda species is reactive for hydrolysis as a deactivation reaction (and also bimolecular deactivation, see above).

Decomposition of Higher Ni(II)-Alkyls. As outlined, the bimolecular homocoupling of Ni(II)-methyl moieties to ethane is a relevant decomposition pathway specific to precursor Ni(II)-methyl complexes. This raises the question for a corresponding reactivity of higher alkyls, Ni(II)-R

(19) An averaged value of 1.9×10^{-4} M^{-1} s^{-1} was calculated independently for $k_{hydr,\mathbf{1}\text{-tmeda}}$ from initial rates of methane formation r_{CH3D} and initial concentrations of **1**-tmeda and D_2O according to $k_{hydr,\mathbf{1}\text{-tmeda}} = r_{CH3D}/([\mathbf{1}\text{-tmeda}]_{t=0}[D_2O]_{t=0})$.

(20) Comparison of the average value of 2.4 × 10−4 s^{-1} for $k_{ins,Me,\mathbf{1}\text{-tmeda}}$ with $k^*_{ins,Me,\mathbf{1}\text{-dmso}} \approx 4.5 \times 10{-}4$ s^{-1} at [C_2H_4] ≈ 0.1 M (calculated from $k_{ins,Me,\mathbf{1}\text{-dmso}} = 6.8 \times 10{-}4$ s^{-1} at [C_2H_4] ≈ 0.15 M; see ref 13) indicates that activation of **1**-tmeda may occur preferentially from **1**-dmso instead of **1**-κ^2-tmeda under the conditions studied. Considering **1**-κ^2-tmeda as a dormant and **1**-dmso as a reactive component toward ethylene under the conditions studied, independent calculation of a corrected pseudo-first-order insertion rate constant according to $k_{ins,Me,\mathbf{1}\text{-tmeda}} = k^*_{ins,Me,\mathbf{1}\text{-dmso}}$ $(1/(1 + [\text{tmeda}]_{free}\{K_{Me}(328\text{ K})[\text{dmso-}d_6]\}^{-1}))$ yields $k^*_{ins,Me,\mathbf{1}\text{-tmeda}} = 3.4 \times 10^{-4}$ s^{-1} ([**1**-tmeda]$_{t=0}$ = 34 mM; [dmso-d_6] = 14.14 M; $K_{Me}(328\text{ K}) = 1.2 \times 10^{-2}$).

(R > Me), which are the active species in ethylene polymerization. In the absence of tmeda,[13] a homocoupling of higher Ni(II)-alkyl moieties had not been observed (but higher Ni(II)-alkyls coupled with Ni(II)-Me present). However, the formation of alkanes from the bimolecular coupling reaction of Ni(II)-alkyl with Ni(II)-hydride species, formed by β-H elimination, was found to be a relevant deactivation pathway intrinsic to neutral Ni(II) catalysts. In view of the specific involvement of tmeda coordination in deactivation reactions of Ni(II)-Me species, namely, both bimolecular elimination of ethane and hydrolysis, the effect of tmeda on deactivation of the active species occurring during polymerization was studied.

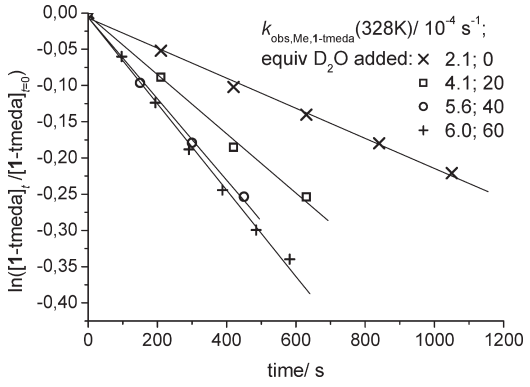

Figure 3. Pseudo-first-order plots of the time-dependent decrease of **1**-tmeda in the presence of ethylene and 0 to 60 equiv of D_2O (pseudo-first-order rate constants $k_{obs,Me,\mathbf{1}\text{-tmeda}}$ determined by linear regression); 34 mM **1**-tmeda, ~0.1 M ethylene.

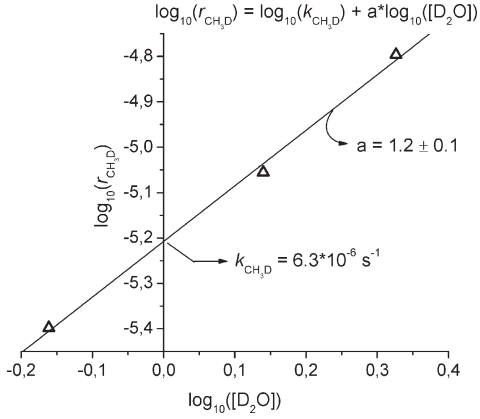

Figure 4. Concentration dependence of observed initial rates of hydrolysis r_{CH3D} on added water as a plot of $\log_{10}(r_{CH3D})$ vs $\log_{10}([D_2O])$ ([**1**-tmeda]$_{t=0}$ = 34 mM, $[D_2O]$ = 0.69, 1.38, and 2.12 M, T = 55 °C).

The gradual formation of CH_4 and C_2H_6 was observed from solutions of dmso- and tmeda-coordinated Ni(II)-methyl and Ni(II)-ethyl species in the presence of ethylene under nonaqueous reaction conditions at T=55 °C (see ^{1}H NMR spectrum at the top of Figure 5). The addition of increasing amounts of water (D_2O) resulted in the formation of CH_3D (see above) in addition to CH_4 and C_2H_6 (see ^{1}H NMR spectrum at the bottom of Figure 5), but no hydrolysis products of higher Ni(II)-alkyl species, e.g., C_2H_5D, were detected.

Summary and Conclusion

The NMR spectroscopic studies reported reveal the very specific nature and reactivity of tmeda-coordinated salicylaldiminato Ni(II)-alkyl complexes, which are highly reactive and versatile intermediates for preparative organometallic chemistry as well as olefin polymerization catalysis.

The NMR spectrocopic studies of the Ni(II)-methyl complex **1**-tmeda reported are consistent with two relevant binding modes of tmeda, an open κ^1- and, unexpectedly, a chelating κ^2-coordination fashion (Scheme 1), which are in equilibrium with each other and the solvent species **1**-L (L = dmso, methanol) and interconvert slowly on the NMR chemical shift time scale. The position of the equilibria depends on the solvent properties, σ-donor ability and polarity, and the temperature. Coordination in a chelating κ^2-fashion renders the salicylaldimine κ^1-O-coordinate. That tmeda is κ^2-coordinate under these conditions is somewhat suprising in view of the lability of tmeda toward other ligands such as pyridine or phosphines, in combination with the finding that even an excess of the latter (monodentate) ligands does not result in displacement of the imine moiety.[7c–7m]

The exposure of dmso solutions of **1**-tmeda to ethylene in an NMR tube resulted in the partial reaction of **1**-tmeda (at a very low degree of conversion of ~10% of Ni(II)-methyl) to form propylene and the dmso- and tmeda-coordinated Ni(II)-ethyl species **2**-dmso and **2**-κ^2-tmeda at 55 °C, which

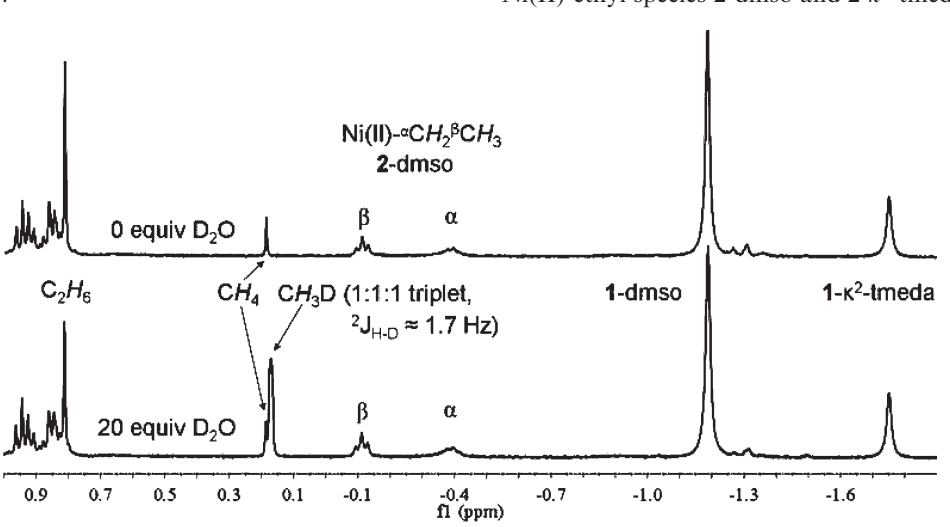

Figure 5. Formation of the decomposition products CH_4 (CH_3D) and C_2H_6 of Ni(II)-alkyls prepared from the reaction of **1**-tmeda with C_2H_4 in the absence (presence) of water (20 equiv of D_2O; bottom spectrum) at T = 55 °C in the NMR tube.

were observed in a close to 1:1 equilibrium mixture after cooling of the sample to 25 °C, demonstrating that κ^2-coordination of tmeda is a relevant binding mode also in higher Ni(II)-alkyl species. Ethylene is catalytically dimerized to butenes. The interconversion of $^{\alpha}$C and $^{\beta}$C moieties of **2**-κ^2-tmeda apparently proceeds slowly as compared to the corresponding interconversion observed for **2**-dmso and the ligand exchange of tmeda vs dmso between the Ni(II)-ethyl species. Studies of the binding affinities of tmeda toward Ni(II)-alkyls in dmso-d_6 (methanol-d_4) solution, quantified as the equilibrium constants $K_{Me}(T)$ and $K_{Et}(T)$ by variable-temperature ^{1}H NMR spectroscopy, showed that the coordination of tmeda is favored by ~2−3 oders of magnitude over the solvent complexes for temperatures from 25 to 55 °C. Overall, by comparison to the analogous tmeda-free system,[13] the formation of tmeda complexes merely retards the ethylene insertion reactions, for which the κ^2-tmeda species appear to be unreactive, i.e., dormant. However, tmeda specise are actively involved in deactivation reactions.

Bimolecular coupling of Ni(II)-methyl moieties to ethane is a relevant deactivation pathway of **1**-tmeda under the reaction conditions studied. An Eyring analysis of second-order rate constants of ethane formation, $k_{\text{Me-Me,}\mathbf{1}\text{-tmeda}}(T)$, afforded activation parameters $\Delta H^{\ddagger} = 97 \pm 7$ kJ mol^{-1} and $\Delta S^{\ddagger} \approx -5$ J mol^{-1} K^{-1}. These differ substantially from $\Delta H^{\ddagger} = 57 \pm 1$ kJ mol^{-1} and $\Delta S^{\ddagger} = -(129 \pm 2)$ J mol^{-1} K^{-1} in the absence of tmeda. This demonstrates that dissociation of coordinated tmeda presumably occurs in a concerted fashion with the rate-determining step of the overall reductive coupling reaction. A tentative explanation for the higher enthalpy is the need for breaking of Ni−N bonds to tmeda, which is partly compensated by the degrees of freedom gained by opening of the rigid five-membered κ^2-tmeda chelate.

In the presence of water, hydrolysis of the Ni(II)−Me bond occurs to a significant extent in dmso solutions of **1**-tmeda. This contrasts with the behavior of the analogous tmeda-free system, for which no substantial hydrolysis occurred under identical conditions. Likely, the hydrogen-bonding capability of free amine moieties is relevant, e.g., interaction with water in the intermediate **1**-κ^1-tmeda (or in **1**-κ^2-tmeda) could promote water coordination and hydrolysis. Quantitative kinetic data of the time-dependent formation of methane (r_{CH3D}) from aqueous (D_2O) dmso-d_6 solutions of **1**-tmeda in the presence of ethylene at T = 55 °C are consistent with a rate law $r_{CH3D} = k_{\text{hydr,}\mathbf{1}\text{-tmeda}}$[**1**-tmeda][$D_2O$], $k_{\text{hydr,}\mathbf{1}\text{-tmeda}} = 1.9 \times 10^{-4}$ M^{-1} s^{-1} ($\Delta G^{\ddagger}$ = 113 kJ mol^{-1} for [**1**-tmeda]$_{t=0}$ = 34 mM). Splitting of observed pseudo-first-order rate constants for the disappearance of the total Ni(II)-methyl resonance of **1**-tmeda (as the sum of **1**-dmso and **1**-κ^2-tmeda) into the contributions of ethylene insertion and Ni(II)−methyl bond hydrolysis according to $k_{\text{obs,Me,}\mathbf{1}\text{-tmeda}} = k_{\text{ins,Me,}\mathbf{1}\text{-tmeda}} + k_{\text{hydr,}\mathbf{1}\text{-tmeda}}[D_2O]$ confirmed that the insertion rate constant $k_{\text{ins,Me,}\mathbf{1}\text{-tmeda}}$ is invariant irrespective of the absence or presence of water.

In contrast to the promotion of irreversible decomposition of Ni(II)-Me complexes in the presence of tmeda by hydrolysis as well as bimolecular coupling of tmeda complexes, no evidence for an analogous enhancement of decomposition of higher alkyl (R > Me) complexes, which are the intrinsic intermediates of polymerization catalysis, was observed under the conditions studied. By contrast to CH_3D formation from **1**-tmeda, no hydrolysis products of higher Ni(II)-alkyl species were observed. Mixtures of Ni(II)-methyl (**1**-κ^2-tmeda and **1**-dmso) and Ni(II)-ethyl species (**2**-κ^2-tmeda and **2**-dmso) gradually decomposed via bimolecular elimination reactions involving either unreacted Ni(II)-methyl or Ni(II)-hydride species to form CH_4 and C_2H_6, consistent with observations of solutions of Ni(II)-alkyls in the absence of tmeda.

In summary, these findings reveal that tmeda, which is introduced in the synthesis of Ni(II) complexes and also in in situ catalysts via the reactive and versatile precursor [(tmeda)Ni(CH_3)$_2$], is not an innocent and relatively weakly coordinating ligand but can displace chelating formally monoanionic ligands and specifically promotes irreversible decomposition of Ni(II)-Me species by hydrolysis as well as bimolecular reductive coupling.

Experimental Section

All manipulations of air- and moisture-sensitive substances were carried out using standard Schlenk, vacuum, and glovebox techniques under argon or dinitrogen. Deuterated solvents (purity and degree of deuteration ≥99.5%) were purchased from Eurisotop. All solvents were thoroughly degassed and saturated with argon prior to use. Dimethyl sulfoxide was distilled from 4 Å molecular sieves or freshly calcined CaO, toluene-d_8 was distilled from a NaK alloy, and methanol-d_4 was used as received. The salicylaldimine (N,O)H, 1-C(H)=NAr-2-OH-3,5-$I_2C_6H_2$ (Ar = 2,6-(3,5-$(F_3C)_2C_6H_3)_2C_6H_3$), and **1**-tmeda were prepared by modification of reported procedures.[7h] [(tmeda)NiMe_2] was purchased from MCAT (Konstanz) and stored at −30 °C in a glovebox. Ethylene of 3.5 grade supplied by Gerling Holz + Co was used as received. NMR spectra were recorded on a Varian Inova 400 spectrometer equipped with either a direct or indirect detection broadband probe, or a Bruker Avance DRX 600 instrument equipped with an H/C/N-TXI inverse probe. ^{1}H and ^{13}C chemical shifts were referenced to residual proton and the naturally abundant ^{13}C resonance of the deuterated solvent, respectively. Assignments of chemical shifts are based on ^{1}H, ^{13}C{^{1}H}, DQF-COSY, ^{1}H,^{13}C-HSQC, ^{1}H,^{13}C-HMBC, ROESY, NOESY, and TOCSY NMR spectra. In order to avoid TOCSY artifacts during ROESY, a 180_x-180_{-x} spin lock scheme was employed.[21] When necessary, high-intensity signals of the solvent, tmeda, and butenes were suppressed by presaturation[22] at multiple irridiation frequencies and/or WATERGATE.[23] An overall recycle delay of 7 and 5 s was applied for the collection of ^{1}H and ^{13}C NMR spectroscopic data, respectively. In general, variable-temperature NMR spectroscopy was carried out with prior temperature determination using a sample of neat methanol ($T \leq 40$ °C) or ethylene glycol ($T \geq 40$ °C). NMR spectra were processed and analyzed with MestreNOVA (v5.3.0). Gel permeation chromatography (GPC) was carried out in 1,2,4-trichlorobenzene/0.0125% BHT at 160 °C at a flow rate of 1 mL min^{-1} on a Polymer Laboratories 220 instrument equipped with Olexis columns with differential refractive index, viscosity, and light-scattering (15° and 90°) detectors. Data reported were determined via triple detection employing the PL GPC-220 software algorithm. The instrument was calibrated with narrow polystyrene and polyethylene standards; data given are referenced to linear polyethylene. Differential scanning calorimetry (DSC) was measured on a Netzsch DSC 204 F1 instrument with a heating/cooling rate of 10 K min^{-1}. DSC data reported are from second heating cycles.

Characterization of 1-κ^2-tmeda. ^{1}H NMR (dmso-d_6, 600 MHz, 25 °C): δ 11.08 (s, 1H, H7); 8.24 (br s, 4H, H15, 21, 23, 29); 7.90 (br s, 2H, H18, 26); 7.77 (d, $^3J_{H-H}$ = 7.6 Hz, 2H,

(21) Hwang, T.-L.; Shaka, A. J. *J. Am. Chem. Soc.* **1992**, *114*, 3157–3159.
(22) (a) Hoult, D. I. *J. Magn. Reson.* **1976**, *21*, 337–347. (b) Schaefer, J. *J. Magn. Reson.* **1972**, *6*, 670–671.
(23) Piotto, M.; Saudek, V.; Sklenar, V. *J. Biomol. NMR* **1992**, *2*, 661–665.

H10, 12); 7.77 (br s, 1H, H6); 7.63 (br s, 1H, H4); 7.48 (br t, $^3J_{H-H}$ =7.6 Hz, 1H, H11); 2.36, 2.01, 1.82, and 1.64 (br s, 3H each, 4× N-CH_3, κ^2-tmeda); 2.09 (obscured by N-methylene protons of free tmeda, N-CH_2−, κ^2-tmeda); −1.79 (s, 3H, Ni(II)-CH_3) ppm. ^{13}C NMR (dmso-d_6, 151 MHz, 25 °C): δ 168.9 (C2); 161.2 (C7); 150.4 (C8); 146.9 (C4); 141.3 (C14, 22); 134.4 (C6), 129.7 (C9, 13); 131.0 (C10, 12); 130.3 (C15, 21, 23, 29); 129.9 (q, $^2J_{C-F}$ =33 Hz, C16, 19, 24, 27); 125.1 (C11); 123.0 (q, $^1J_{C-F}$ = 273 Hz, C17, 20, 25, 28); 120.0 (C18, 26); 118.9 (C1); 99.5 (C3); 73.6 (C5); 60.4 and 54.6 (2× N-CH_2-, κ^2-tmeda); 45.9, 47.5, 45.9, and 48.6 (4× N-CH_3, κ^2-tmeda); −15.0 (Ni(II)-CH_3) ppm.

General Procedure for Quantitative Studies of 1-tmeda by Variable-Temperature ^{1}H NMR Spectroscopy. In typical experiments, a 34 mM dmso-d_6 solution of **1**-tmeda was prepared in an NMR tube sealed with a rubber septum in the glovebox. The tubes were kept at room temperature outside the spectrometer, and NMR spectra were acquired with the NMR probe prewarmed to desired temperatures. Relative concentrations were determined from integration of the respective resonances and normalization to an integral value for Ni(II)-CH_3 = 1 ([**1**-tmeda]$_{t=0}$ = 34 mM; [dmso-d_6] = 14.14 M). Equilibrium constants were calculated from ^{1}H NMR spectra, linear regression of plots of ln(K(T)) vs reciprocal temperatures yielded reaction enthalpies $\Delta H°$, and free reaction enthalpies $\Delta G°$ were calculated from equilibrium constants at 25 °C. Water ([D_2O] in the range from 0.69 to 1.38 and 2.12 M equal to 20, 40, and 60 equiv per **1**-tmeda) and ethylene (3−4 mL) were added via gastight syringes. The gradual disappearance of the Ni(II)-CH_3 resonances of **1**-tmeda was monitored at T = 55 °C after ethylene addition. Linear regression yielded values of $k_{obs,Me,\mathbf{1}\text{-tmeda}}$ (from plots of ln([**1**-tmeda]$_t$/[**1**-tmeda]$_{t=0}$) vs time) and the reaction order with respect to water and $k_{hydr,\mathbf{1}\text{-tmeda}}$ (from a plot of $\log_{10}(r_{CH3D})$ vs $\log_{10}([D_2O])$).

General Procedure for the Kinetic Analysis of Ethane Formation from 1-tmeda. NMR samples of **1**-tmeda in dmso-d_6 (34 mM) were prepared in a glovebox. Tubes were sealed with a rubber septum and removed from the glovebox. Samples were inserted into the prewarmed NMR probe and the decrease of the total Ni(II)-CH_3 resonance (as the sum of **1**-dmso and **1**-κ^2-tmeda) was followed with time by ^{1}H NMR spectroscopy for temperatures from 55 to 80 °C. Integral values were normalized to the value at t = 0 and converted into concentrations by multiplication with the starting concentration of **1**-tmeda. Second-order rate constants $k_{Me\text{-}Me,\mathbf{1}\text{-tmeda}}(T)$ were calculated from linear regression of plots of $1/[\mathbf{1}\text{-tmeda}]_t - 1/[\mathbf{1}\text{-tmeda}]_{t=0}$ vs time. Linear regression of a plot of $\ln\{k_{Me_2Me,\mathbf{1}\text{-tmeda}}(T)/T\}$ vs $1/T$ provided the activation parameters $\Delta H^{\ddagger}$ and $\Delta S^{\ddagger}$.

Acknowledgment. Financial support by the DFG (Me1388/3-2) is gratefully acknowledged. We thank Anke Friemel for technical support and Lars Bolk for GPC and DSC measurements. S.M. is indebted to the Fonds der Chemischen Industrie and to the Hermann Schnell-Foundation.

Supporting Information Available: General procedure of high-pressure polymerization experiments, NMR spectra of **1**-κ^2-tmeda and **2**-κ^2-tmeda in dmso-d_6 solution, and plots for the determination of kinetic and thermodynamic data obtained from NMR spectroscopic studies. This material is available free of charge via the Internet at http://pubs.acs.org.